

Electronic Supplementary Information (ESI)

A colorimetric and ‘OFF-ON’ fluorometric chemosensor based on Rhodamine-pyrazole derivative for the detection of Al^{3+} , Fe^{3+} and Cr^{3+} metal ions, and its intracellular application†

Sarita Gond^a, Pranjalee Yadav^a, Aayoosh Singh^a, Somenath Garai^a, Anusmita Shekher^b, Subash Chandra Gupta^{b,c}, Vinod P. Singh^{a*}

*E mail: singvp@yahoo.co.in

^aDepartment of Chemistry, Institute of Science, Banaras Hindu University, Varanasi 221005, India

^bDepartment of Biochemistry, Institute of Science, Banaras Hindu University, Varanasi 221005, India

^cDepartment of Biochemistry, All India Institute of Medical Sciences, Guwahati, Assam, India

TABLE OF CONTENTS

	General procedures
Fig. S1	¹ H NMR spectrum of Rhodamine B hydrazide
Fig. S2	¹³ C NMR spectrum of Rhodamine B hydrazide
Fig. S3	IR spectrum of Rhodamine B hydrazide
Fig. S4	¹ H NMR spectrum of RMP
Fig. S5	¹³ C NMR spectrum of RMP
Fig. S6	Mass spectrum of RMP
Table S1	Bond lengths in Å for RMP
Table S2	Bond angles for RMP
Fig. S7	Mass spectrum of RMP-Al ³⁺
Fig. S8	Mass spectrum of RMP-Fe ³⁺
Fig. S9	Mass spectrum of RMP-Cr ³⁺
Fig. S10	Absorption studies of RMP (20 μM) on pH 6 to 1 in ethanol/HEPES (7:3, v/v) buffer
Fig. S11	(a) Color change of RMP (20 μM) in the presence of other cations in visible light (b) UV-visible spectra of RMP (20 μM) in ethanol/HEPES (7:3, v/v; pH 7.2) buffer solution on addition of different metal ions (c) expanded form of Al ³⁺ , Fe ³⁺ and Cr ³⁺ metal ions
Fig. S12	Fluorescence response of RMP (20 μM, λ _{ex} = 510 nm) in ethanol/HEPES (7:3, v/v; pH 7.2) buffer upon addition of various metal ions (20 μM) in presence of (a) Al ³⁺ , (b) Fe ³⁺ and (c) Cr ³⁺
Fig. S13, S14	(a) Fluorescence spectra of RMP (20 μM, λ _{ex} = 510 nm) in ethanol/HEPES (7:3, v/v; pH 7.2) buffer solution, showing change in emission intensity at 575 nm with incremental addition of Fe ³⁺ /Cr ³⁺ metal ions (b) reversibility test of RMP toward Fe ³⁺ /Cr ³⁺ by using EDTA
Fig. S15	Job's plots of RMP for Fe ³⁺ and Cr ³⁺
Fig. S16, S17	Binding constants and Limits of detection of RMP for Fe ³⁺ and Cr ³⁺
Table S3	Comparison with previously reported sensors
Fig. S18	Effect of RMP on the viability of SiHa cells.
	References

General procedures

UV-Vis and fluorescence spectral studies

Job's plot, UV-visible, and fluorescence titration studies were performed using a 20 μM acetonitrile solution of **RMP** at room temperature. Milli-Q water was used as solvent for making the metal ion solutions. The binding stoichiometry between **RMP** and metal ions were computed from Job's plot, and binding constants (K_a) of **RMP** for Al^{3+} , Fe^{3+} and Cr^{3+} were calculated by using Benesi-Hildebrand equation (1).¹

$$(I_0/I - I_0) = (a/b-a)(1/Ka[\text{Metal}]+1) \quad (1)$$

where, I and I_0 represent the fluorescence intensities of **RMP** at 510 nm in the presence and absence of metal ion ; a and b are constants.

The Detection limit (LOD) for **RMP** was computed with the help of equation (2). The slope was acquired from a linear fitting plot of absorbance/fluorescence ratio versus concentration of metal ions added.²

$$\text{LOD} = 3\sigma/\text{slope} \quad (2)$$

Fluorescence quantum yield measurements

The following equation is used to figure out the amount of fluorescence given off by **RMP** and its M^{3+} complexes:

$$Q = Q_r(I/I_r) \times (OD_r/OD) \times (n^2/n_r^2) \quad (3)$$

Where Q and I represent the quantum yield and integrated fluorescence intensity of the fluorescence, respectively. The solvent's refractive index and absorbance are represented by the symbols n and OD , respectively. Reference quinine sulphate (indicated by r) has a quantum yield of 0.54 in 0.5 M H_2SO_4 . Quantum yield is determined by integrating the area of the emission spectrum using the instrument's built-in software.

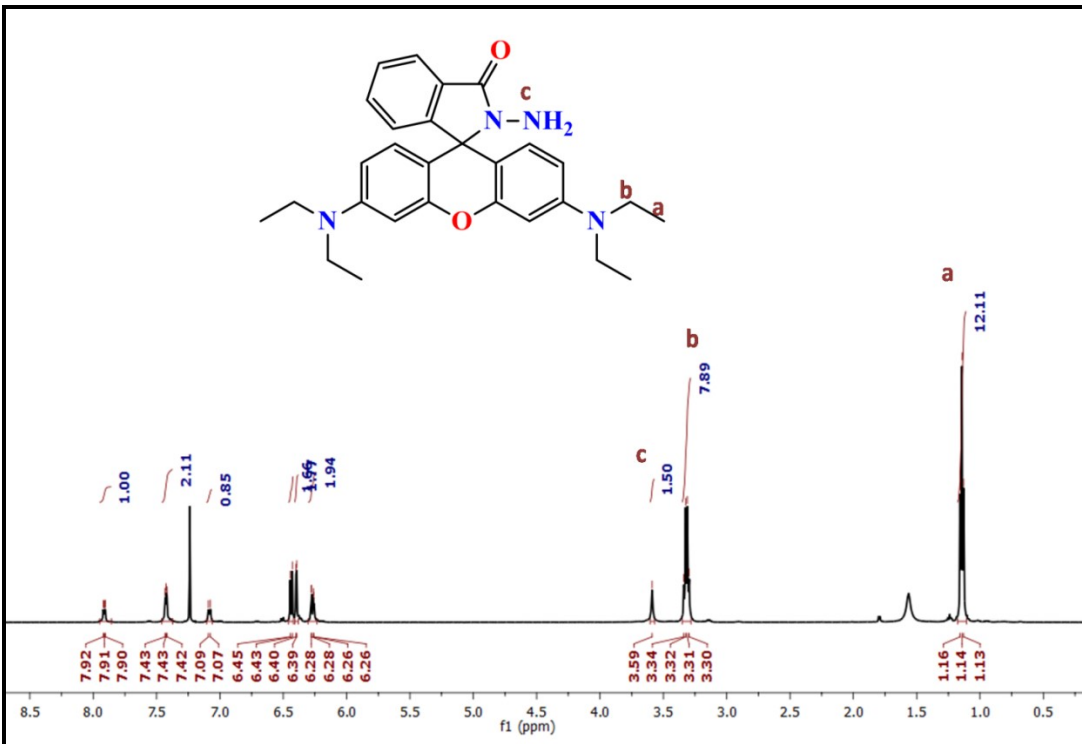


Fig. S1 ^1H NMR spectrum of Rhodamine B hydrazide

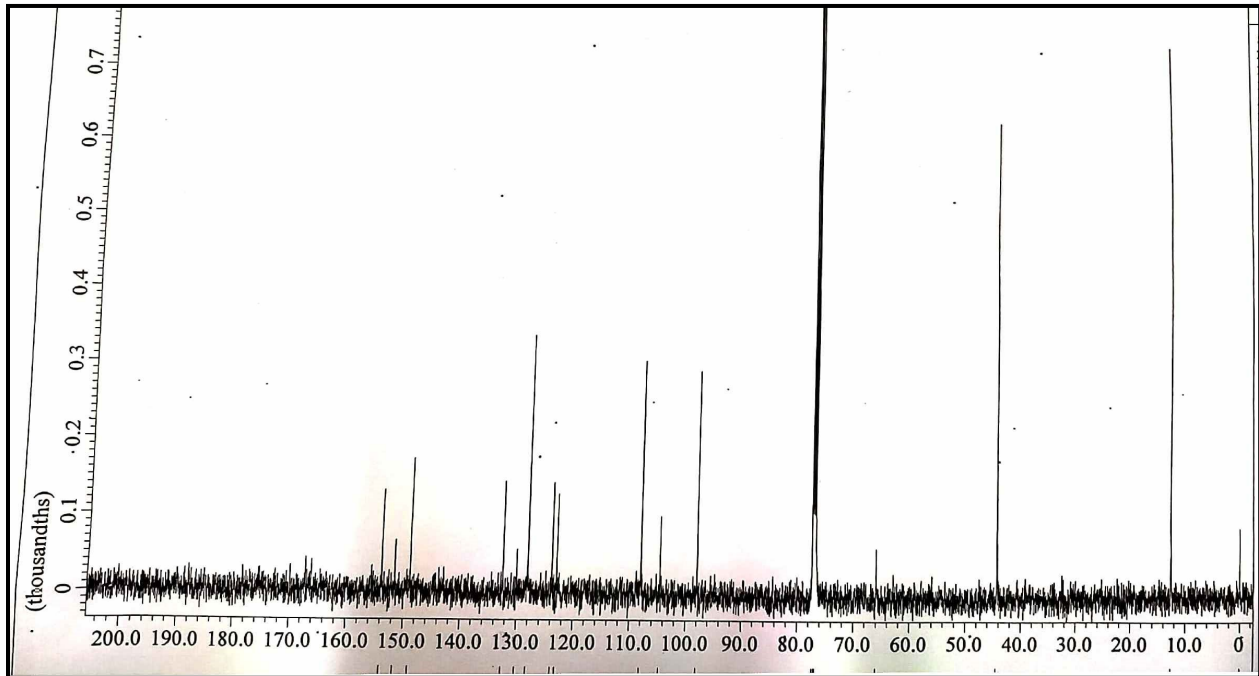


Fig. S2 ^{13}C NMR spectrum of Rhodamine B hydrazide

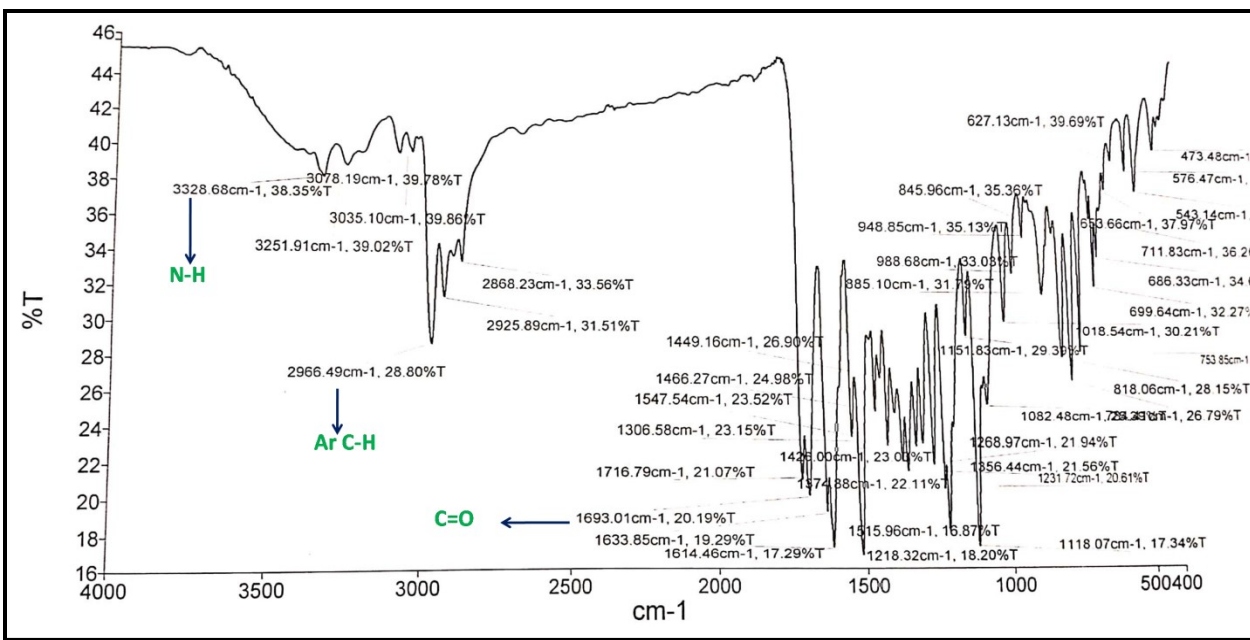


Fig. S3 IR spectrum of Rhodamine B hydrazide

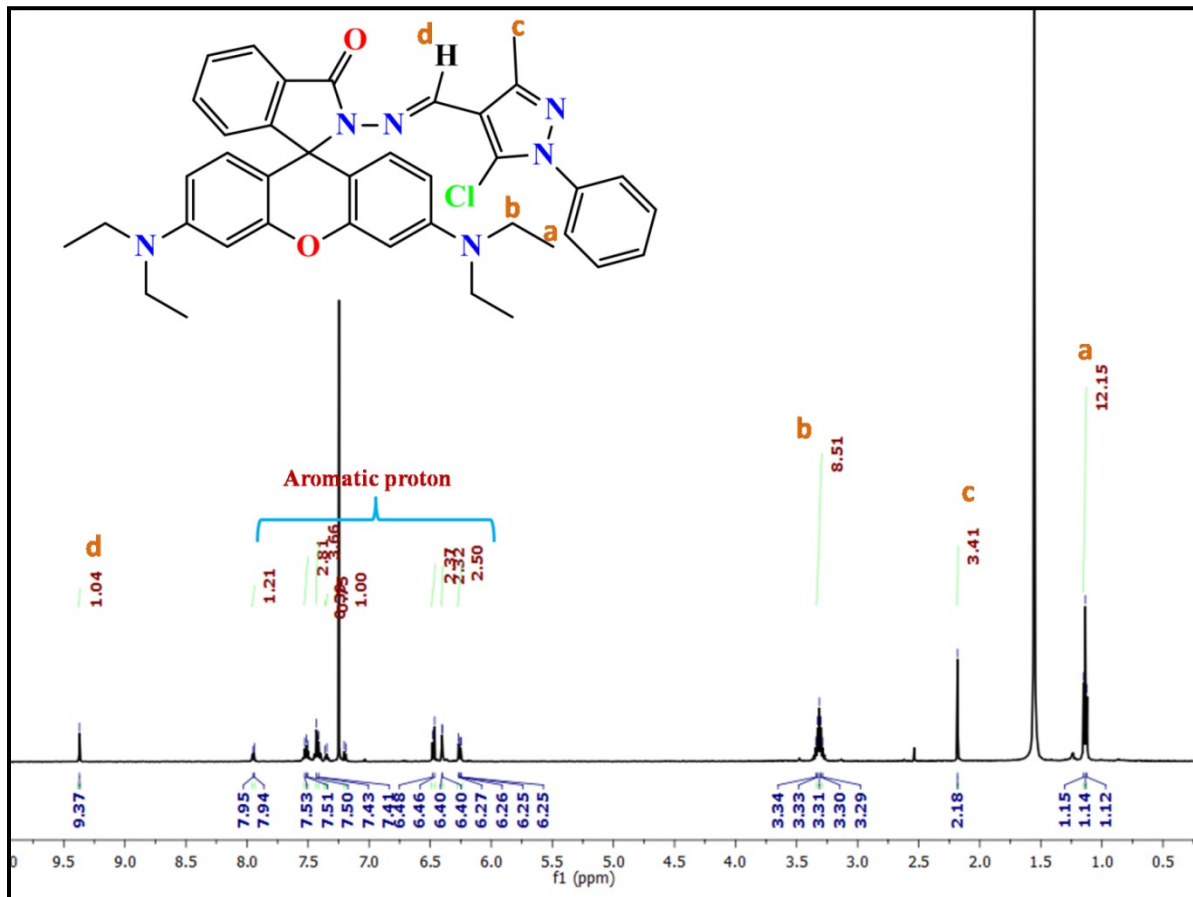


Fig. S4 ¹H NMR spectrum of RMP

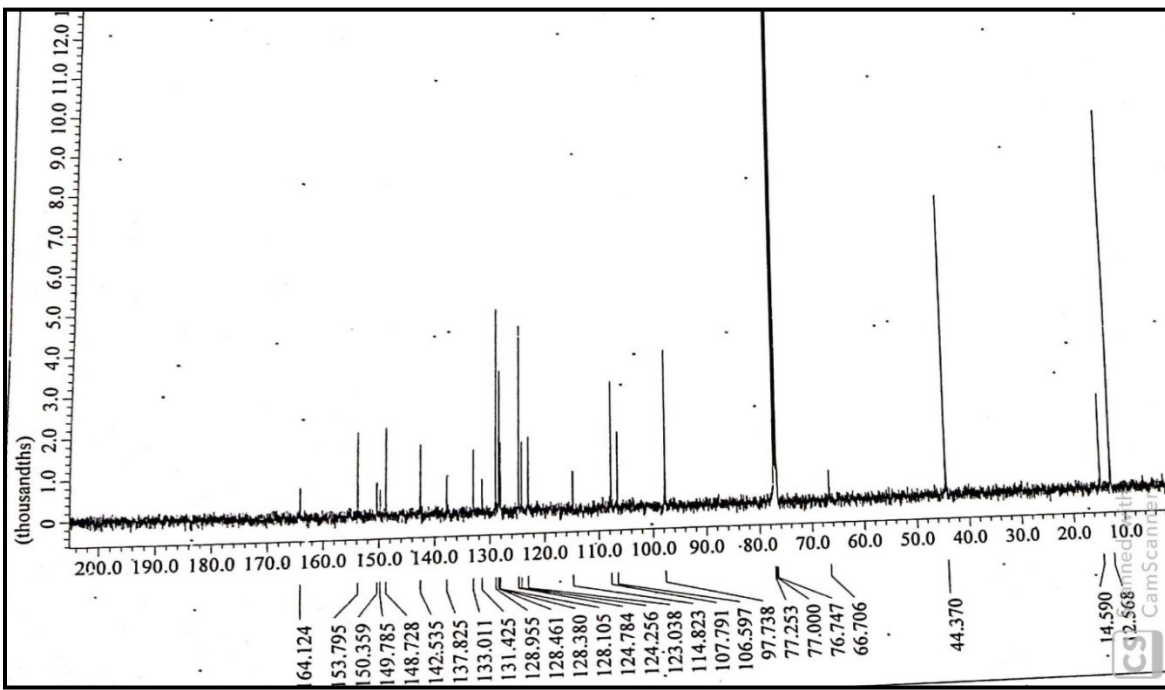


Fig. S5 ^{13}C NMR spectrum of RMP

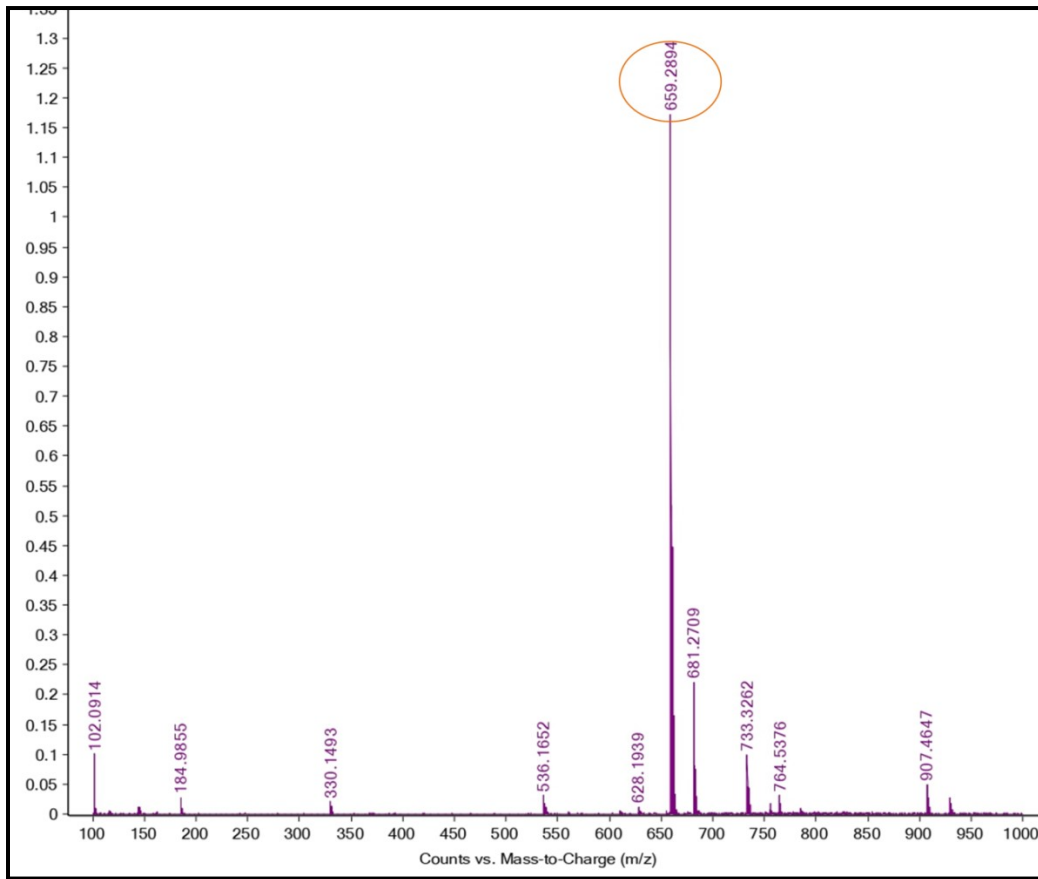


Fig. S6 Mass spectrum of RMP

Table S1 bond lengths in Å for RMP

Bond length (Å)			
C1-C38	1.765(7)	C28-C32	1.397(5)
O1-C4	1.388(4)	C30-C44	1.393(5)
O1-C6	1.369(4)	N5-C40	1.307(7)
N1-N4	1.377(3)	C34-C41	1.444(5)
N1-C34	1.273(4)	C36-C46	1.389(5)
O2-C16	1.229(4)	C38-C41	1.316(7)
N4-C10	1.486(3)	C40-C27	1.524(7)
N4-C16	1.370(4)	C40-C41	1.295(7)
C1-C4	1.385(4)	C42-C48	1.478(6)
C1-C10	1.509(4)	C44-C50	1.349(7)
C1-C20	1.383(4)	C46-C50	1.393(8)
C4-C28	1.355(4)	C25-C35	1.415(11)
C6-C8	1.376(4)	C13-C17	1.340(8)
C6-C14	1.390(4)	C7-C29	1.3900
C8-C10	1.516(4)	C7-C33	1.3900
C8-C12	1.382(4)	C29-C15	1.3900
N6-N5	1.323(7)	C15-C31	1.3900
N6-C38	1.300(9)	C31-C2	1.3900
N6-C2	1.465(7)	C2-C33	1.3900
C10-C22	1.528(4)	C9-C37	1.42(2)
C12-C24	1.373(5)	C19-C39	1.60(2)
C14-C18	1.401(5)	N3-C5	1.504(5)
C16-C30	1.454(5)	N3-N7	1.505(5)
C18-C24	1.403(5)	N3-C47	1.339(10)
C18-N2	1.376(5)	C5-C41	1.505(5)
C20-C26	1.367(5)	C5-Cl2	1.395(8)
C22-C30	1.380(5)	C41-C21	1.505(5)
C22-C36	1.366(5)	C21-N7	1.504(5)
N8-C32	1.370(5)	C21-C43	1.445(15)
N8-C25	1.437(6)	C11-C45	1.3900
N8-C13	1.488(7)	C11-C49	1.3900
C26-C32	1.402(5)	C45-C23	1.3900
N2-C42	1.447(5)	C23-C47	1.3900
N2-C9	1.486(16)	C47-C3	1.3900
N2-C19	1.503(18)	C3-C49	1.3900

Table S2 bond angles for RMP

Bond angle ($^{\circ}$)			
C6-O1-C4	118.8(2)	N1-C34-C41	119.2(3)
C34-N1-N4	119.6(3)	C16-N4-C10	114.7(2)
N1-N4-C10	114.95(19)	C4-C1-C10	121.6(3)
C16-N4-N1	129.3(3)	C20-C1-C4	115.8(3)
C1-C4-O1	122.5(3)	C20-C1-C10	122.5(2)
C28-C4-O1	114.8(2)	C22-C36-C46	117.1(4)
C28-C4-C1	122.7(3)	N6-C38-C11	120.1(5)
O1-C6-C8	123.2(3)	N6-C38-C41	106.1(6)
O1-C6-C14	114.2(2)	C41-C38-C11	133.7(6)
C8-C6-C14	122.7(3)	N5-C40-C27	124.2(5)
C6-C8-C10	121.8(3)	C41-C40-N5	111.3(4)
C6-C8-C12	115.7(3)	C41-C40-C27	124.5(5)
C12-C8-C10	122.4(2)	N2-C42-C48	114.4(4)
N5-N6-C2	117.3(6)	C50-C44-C30	118.3(4)
C38-N6-N5	111.4(5)	C36-C46-C50	121.8(5)
C38-N6-C2	131.3(5)	C44-C50-C46	120.5(4)
N4-C10-C1	110.4(2)	C35-C25-N8	115.5(8)
N4-C10-C8	109.9(2)	C17-C13-N8	108.3(7)
N4-C10-C22	99.6(2)	C29-C7-C33	120.0
C1-C10-C8	110.7(2)	C15-C29-C7	120.0
C1-C10-C22	112.6(2)	C31-C15-C29	120.0
C8-C10-C22	113.1(3)	C15-C31-C2	120.0
C24-C12-C8	123.4(3)	C31-C2-N6	123.3(4)
C6-C14-C18	121.0(3)	C33-C2-N6	116.7(4)
O2-C16-N4	125.6(3)	C33-C2-C31	120.0
O2-C16-C30	129.0(3)	C2-C33-C7	120.0
N4-C16-C30	105.4(3)	C37-C9-N2	112.5(13)
C14-C18-C24	116.2(3)	N2-C19-C39	100.5(15)
N2-C18-C14	121.4(3)	C5-N3-N7	108.0
N2-C18-C24	122.4(3)	C47-N3-C5	132.5(7)
C26-C20-C1	123.0(3)	C47-N3-N7	119.1(7)
C30-C22-C10	109.7(3)	N3-C5-C41	108.0
C36-C22-C10	129.0(3)	C12-C5-N3	124.7(5)
C36-C22-C30	121.3(3)	C12-C5-C41	125.4(5)
C12-C24-C18	120.9(3)	C34-C41-C5	130.4(3)
C32-N8-C25	122.3(4)	C34-C41-C21	120.9(3)
C32-N8-C13	119.5(4)	C38-C41-C34	119.3(5)
C25-N8-C13	118.0(4)	C40-C41-C34	132.5(4)
C20-C26-C32	120.5(3)	C40-C41-C38	107.6(5)
C18-N2-C42	122.0(3)	C21-C41-C5	108.0
C18-N2-C9	120.5(7)	N7-C21-C41	108.0
C18-N2-C19	117.0(8)	C43-C21-C41	146.1(7)
C42-N2-C9	117.2(7)	C43-C21-N7	105.0(8)
C42-N2-C19	115.6(9)	C21-N7-N3	108.0
C4-C28-C32	121.4(3)	C45-C11-C49	120.0
C22-C30-C16	110.5(3)	C23-C45-C11	120.0
C22-C30-C44	121.1(4)	C47-C23-C45	120.0

C44-C30-C16	128.4(4)	N3-C47-C23	117.1(8)
N8-C32-C26	121.4(3)	N3-C47-C3	122.9(8)
N8-C32-C28	122.0(3)	C23-C47-C3	120.0
C28-C32-C26	116.5(3)	C49-C3-C47	120.0
C40-N5-N6	103.6(5)	C3-C49-C11	120.0

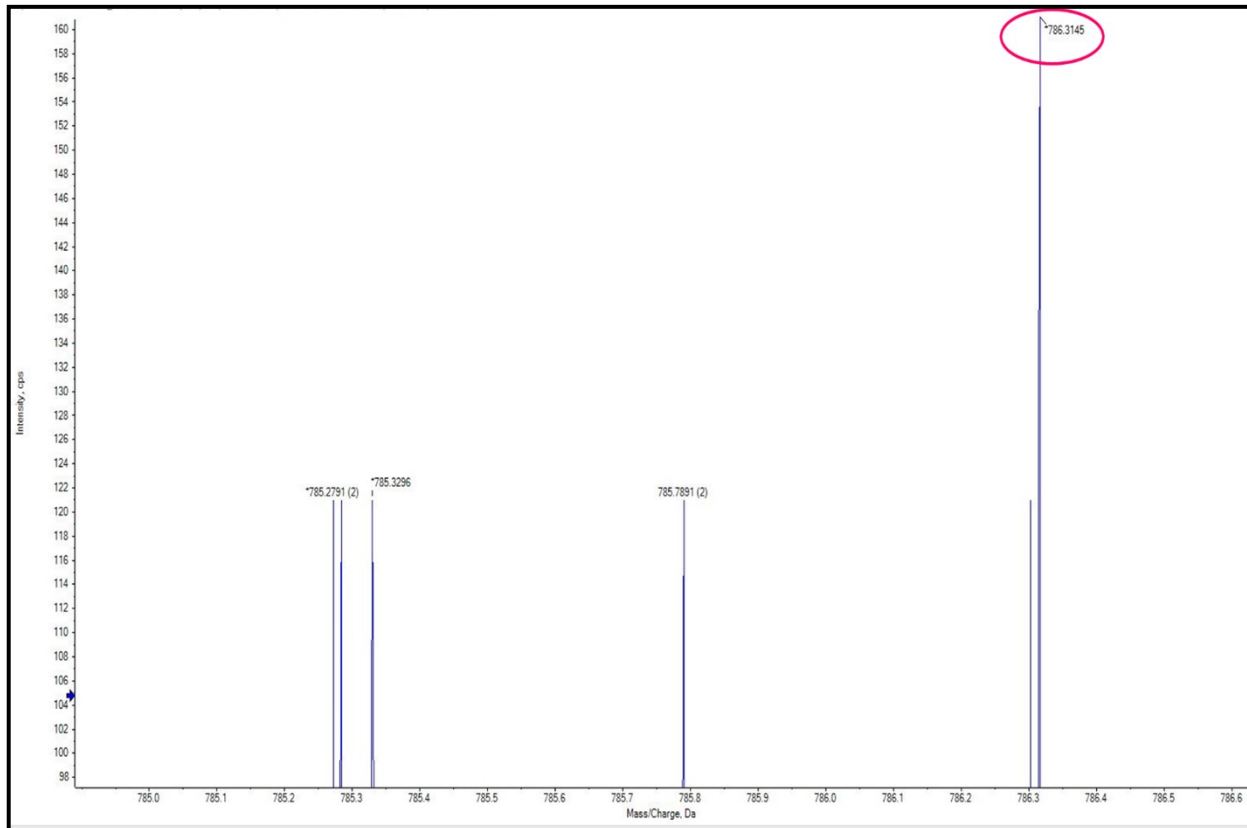


Fig. S7 Mass spectrum of RMP-Al³⁺ complex

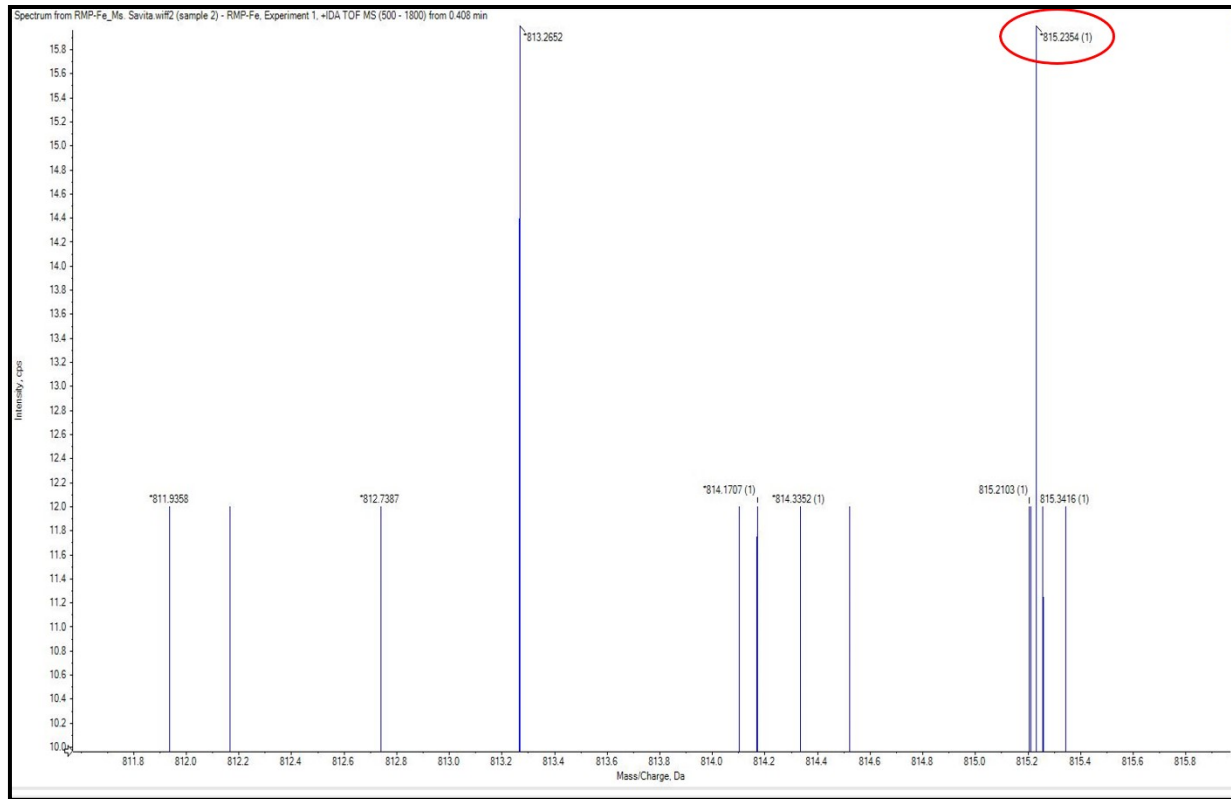


Fig. S8 Mass spectrum of **RMP-Fe³⁺** complex

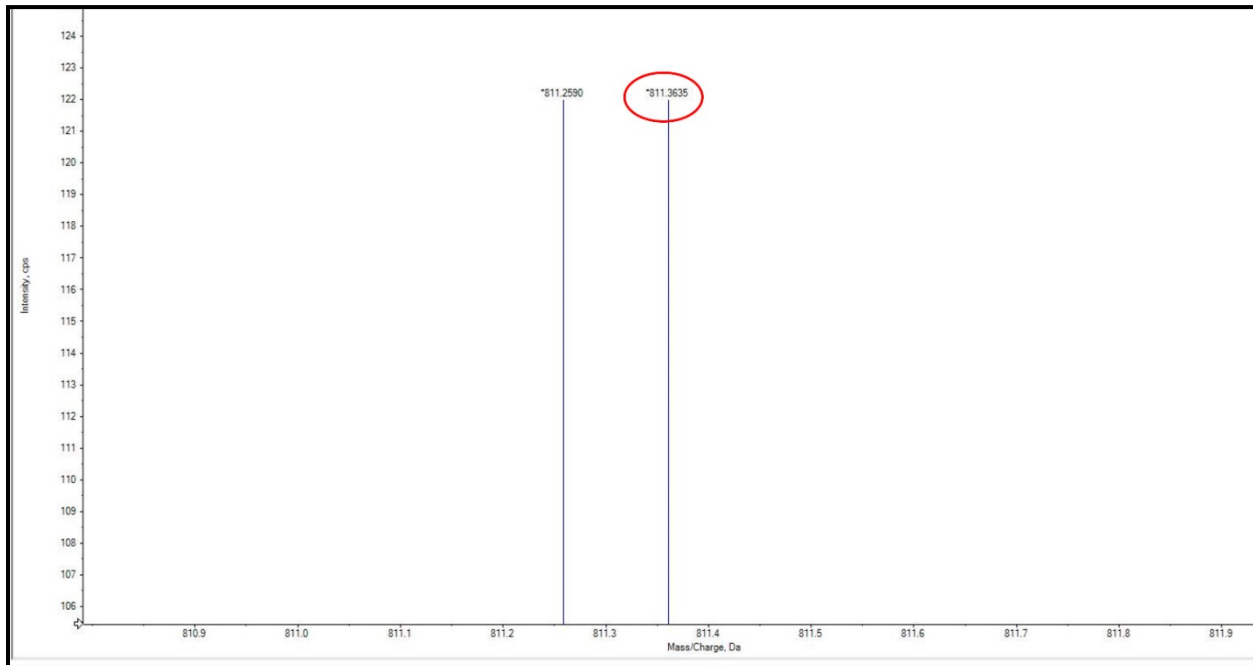


Fig. S9 Mass spectrum of **RMP-Cr³⁺** complex

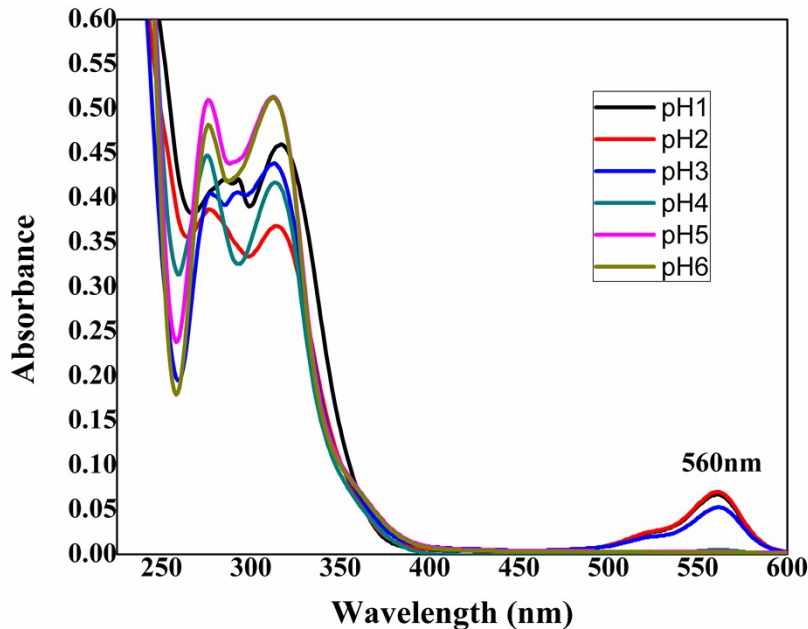


Fig. S10 Absorption studies of RMP (20 μ M) on pH 6 to 1 in ethanol/HEPES (7:3, v/v) buffer solution

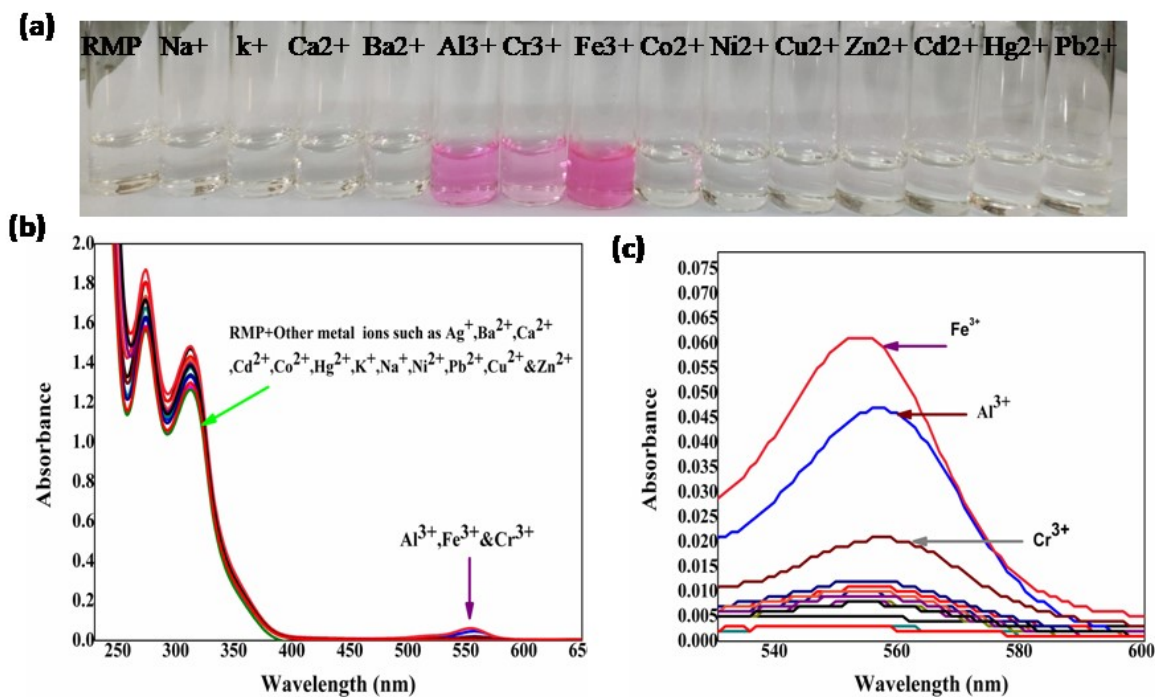


Fig. S11(a) Color change of RMP (20 μ M) in the presence of other cations invisible light**(b)**UV-visible spectra of RMP (20 μ M) in ethanol/HEPES (7:3, v/v; pH 7.2) buffer solution on addition of different metal ions **(c)** expanded form of Al³⁺, Fe³⁺ and Cr³⁺ metal ions

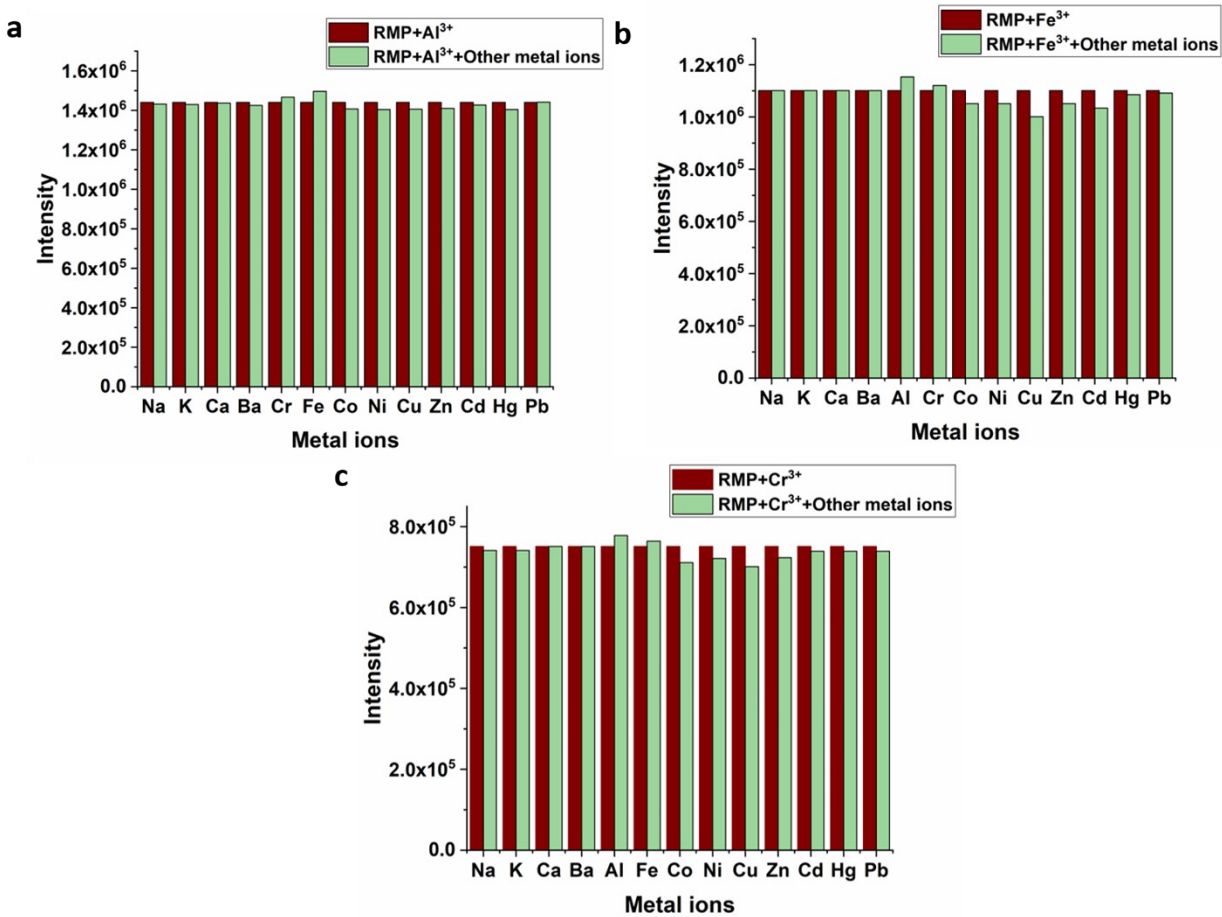


Fig. S12 Fluorescence response of **RMP** (20 μ M, $\lambda_{\text{ex}} = 510$ nm) in ethanol/HEPES (7:3, v/v; pH 7.2) buffer upon addition of various metal ions (20 μ M) in presence of (a) Al^{3+} , (b) Fe^{3+} and (c) Cr^{3+} .

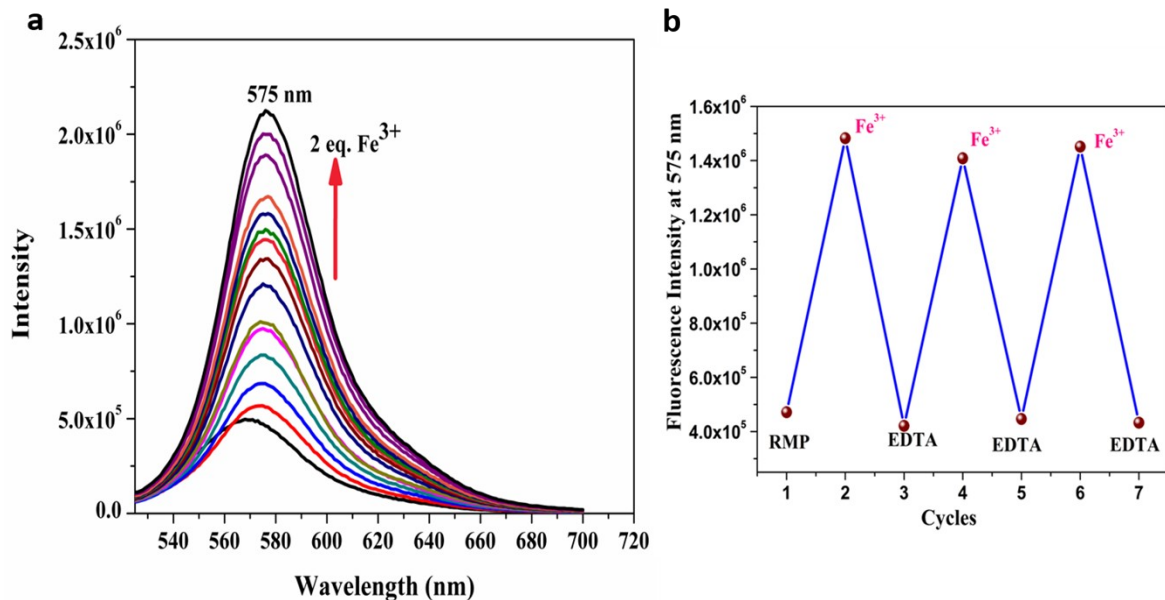
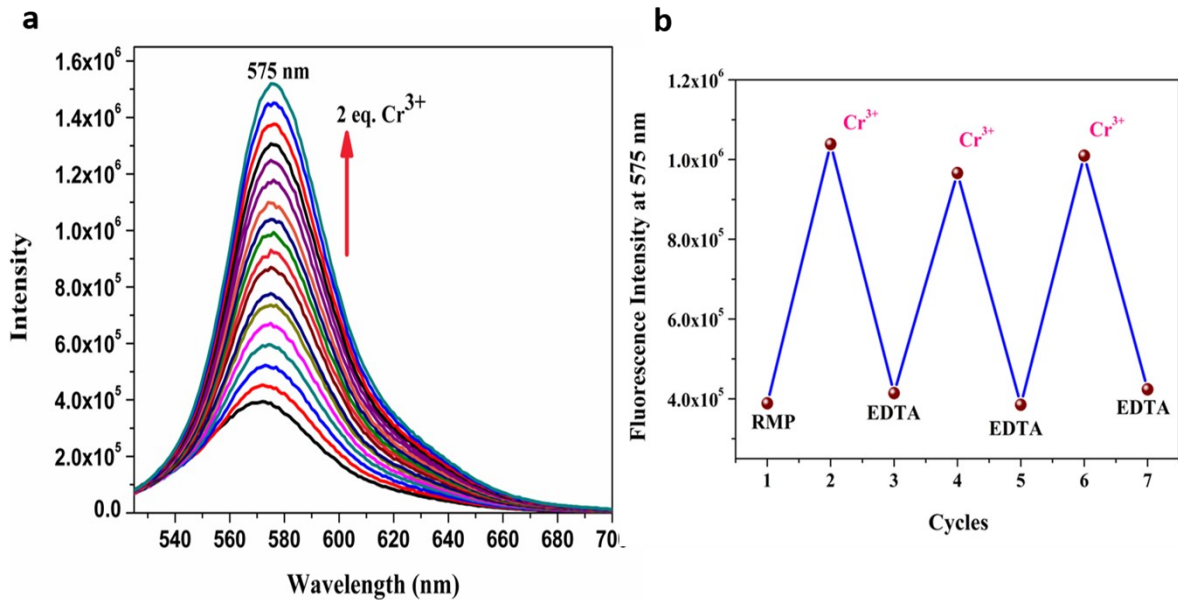


Fig. S13 (a) Fluorescence spectra of **RMP** ($20 \mu\text{M}$, $\lambda_{\text{ex}} = 510 \text{ nm}$) in ethanol/HEPES (7:3, v/v; pH 7.2) buffer solution, showing change in emission intensity at 575 nm with incremental addition of Fe^{3+} metal ion (b) reversibility test of **RMP** toward Fe^{3+} by using EDTA



g. S14 (a) Fluorescence spectra of **RMP** ($20 \mu\text{M}$, $\lambda_{\text{ex}} = 510 \text{ nm}$) in ethanol/HEPES (7:3, v/v; pH 7.2) buffer solution, showing change in emission intensity at 575 nm with incremental addition of Cr^{3+} metal ion (b) Reversibility test of **RMP** toward Cr^{3+} by using EDTA

Fi

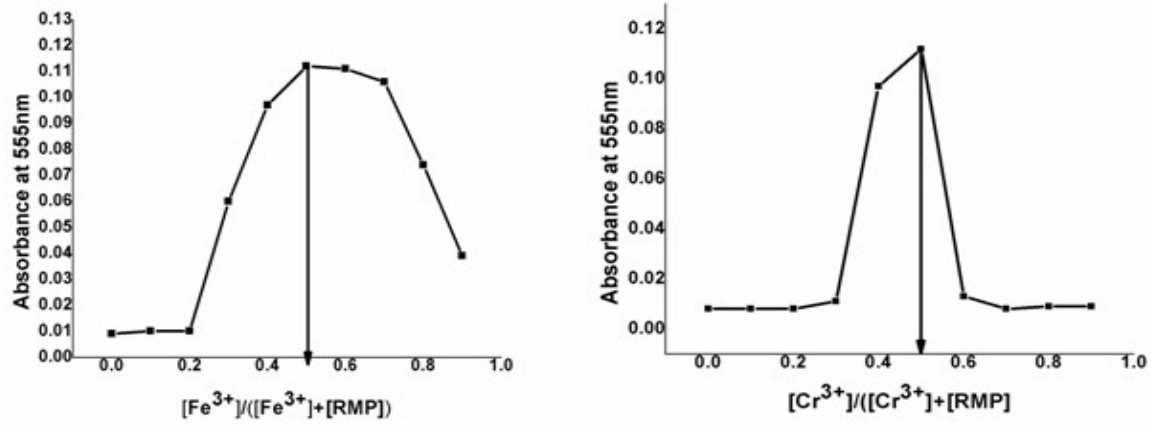


Fig. S15. Job's plots of RMP for Fe³⁺ and Cr³⁺

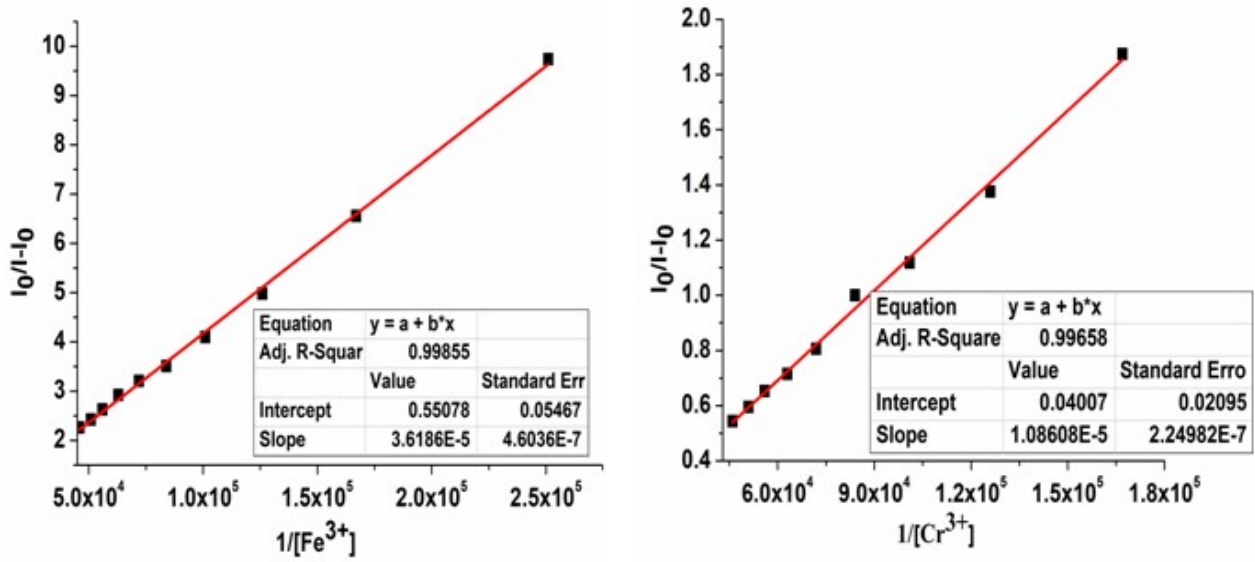


Fig. S16 Binding constants of RMP for Fe³⁺ and Cr³⁺

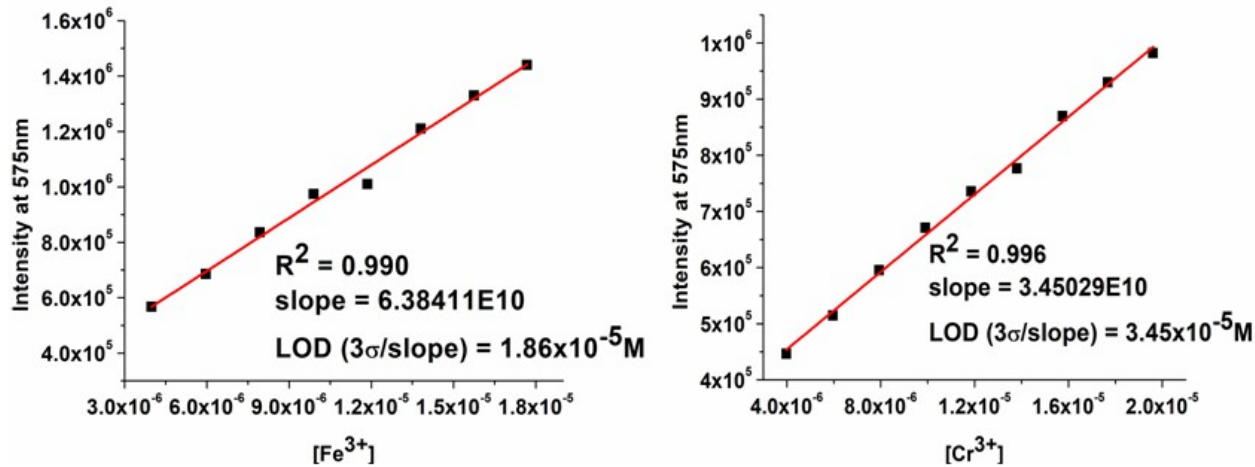


Fig. S17 Limits detection of RMP for Fe^{3+} and Cr^{3+}

Table S3 Comparison with previously reported sensors

S. N.	Wavelength ($\lambda_{\text{ex}}/\lambda_{\text{em}}$) (nm)	Solvent system	Analytes	LOD (M)	Application	Ref.
1.	530/588	$\text{CH}_3\text{OH}/\text{H}_2\text{O}$ (8:2, v/v)	Al^{3+} Fe^{3+} Cr^{3+}	2.7×10^{-3} 1.9×10^{-3} 3.5×10^{-3}	NA	[3]
2.	480/583	Methanol	Al^{3+} Fe^{3+} Cr^{3+}	2.2×10^{-5} 1.4×10^{-5} 6.3×10^{-5}	logic gate	[4]
3.	520/585	$\text{CH}_3\text{OH}/\text{H}_2\text{O}$ (1/3, v/v)	Al^{3+} Fe^{3+} Cr^{3+}	- - -	NA	[5]
4.	314/430	H_2O	Al^{3+} Fe^{3+} Cr^{3+}	1.09×10^{-4} 1.66×10^{-5} 6.17×10^{-5}	NA	[6]
5.	365/470	ethanol/water (2:1, v/v)	Al^{3+} Fe^{3+} Cr^{3+}	2×10^{-4} 8×10^{-5} 1×10^{-4}	NA	[7]
6.	510/575	Ethanol/HEPES buffer(7:3, v/v)	Al^{3+} Fe^{3+} Cr^{3+}	1.74×10^{-5} 3.45×10^{-5} 1.86×10^{-5}	Live cell imaging, molecular logic gate	This work

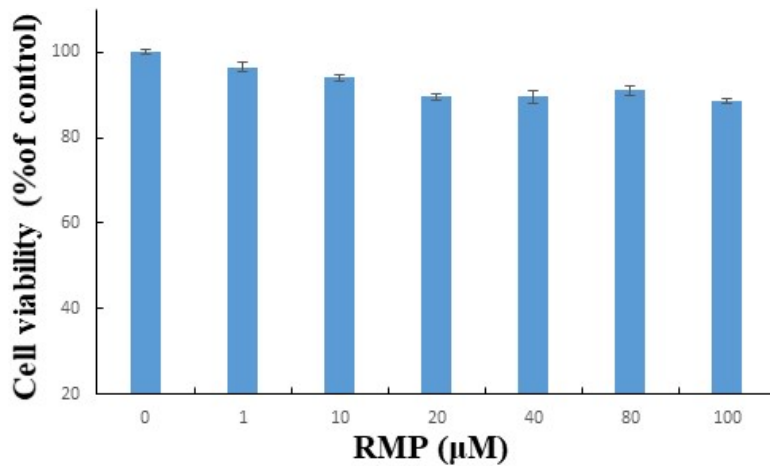


Fig. S18 Effect of **RMP** on the viability of SiHa cells. The cells were treated with indicated concentrations of **RMP** for 24 h in the culture medium at neutral pH. The cell viability was examined by MTT assay

References

- 1 H.A. Benesi and J.H. Hildebrand, *J. Am. Chem. Soc.*, 1949, **71**, 2703–2707.
- 2 G.L. Long and J. D. Winefordner, *Anal. Chem.*, 1983, **55**, 712A–724A.
- 3 S. Hou, Z. Qu, K. Zhong, Y. Bian, L. Tang, *Tetrahedron Letters*, 2016, **57**, 2616-2619.
- 4 X. Yue, C. Li, Z. Yang, *J. Photochem. Photobiol. A: Chemistry*, 2018, **351**, 1-7.
- 5 H. Wang, T. Kang, X. Wang, L. Feng, *Sensors and Actuators B: Chemical*, 2018, **264**, 391-397.
- 6 Z. Zhan, X. Liang, X. Zhang, Y.Jia, M. Hu, *Dalton Trans.*, 2019, **48**, 1786-1794.
- 7 S. Tao, X. Li, C. Wang, C. Meng, *Chemistry Select*, 2016, **1**, 3208–3214.